Vesuvianite from the Somma-Vesuvius Complex: New Data and Revised Formula

Taras L. Panikorovskii [1,2,*] 🆔, **Nikita V. Chukanov** [3], **Vyacheslav S. Rusakov** [4] 🆔, **Vladimir V. Shilovskikh** [5], **Anton S. Mazur** [6], **Giuseppina Balassone** [7] 🆔, **Gregory Yu. Ivanyuk** [2] and **Sergey V. Krivovichev** [1,2]

1   Department of Crystallography, Institute of Earth Sciences, St. Petersburg State University, University Embankment, 7/9, St. Petersburg 199034, Russia; s.krivovichev@spbu.ru
2   Kola Science Centre, Russian Academy of Sciences, 14 Fersman Street, Apatity 184200, Russia; ivanyuk@admksc.apatity.ru
3   Institute of Problems of Chemical Physics, Russian Academy of Sciences, Chernogolovka 142432, Russia; chukanov@icp.ac.ru
4   Faculty of Physics, Moscow State University, Vorobievy Gory, Moscow 119991, Russia; rusakov@phys.msu.ru
5   Department of Colloid Chemistry, Insitute of Chemistry, St. Petersburg State University, University Av. 26, St. Petersburg 198504, Russia; vova_bel@mail.ru
6   Center for Magnetic Resonance, St. Petersburg State University, University Av. 26, St. Petersburg 198504, Russia; a.mazur@spbu.ru
7   Dipartimento di Scienze della Terra, dell'Ambiente e delle Risorse, Università degli Studi di Napoli Federico II, Compless Universitario Monte S. Angelo, Via Cinthia 26, 80126 Napoli, Italy; balasson@unina.it
*   Correspondence: taras.panikorovsky@spbu.ru; Tel.: +7-812-363-69-14

Abstract: At present, the vesuvianite group of minerals consists of eight members, six of which are distinguished by the dominant cation in the $Y1(A,B)$ five-coordinated site. We investigated two vesuvianite samples from the type locality by electron microprobe analysis, Mössbauer and infrared spectroscopy, TGA/DSC, MAS NMR, single-crystal and powder X-ray diffraction. The crystal structures of these samples (# **27844** and **51062** from the Vesuvius collection, Fersman Mineralogical Museum, Moscow) have been refined to $R_1 = 0.027$ and $R_1 = 0.035$, respectively. Both samples have the space group $P4/nnc$; $a = 15.5720(3)$ and $15.5459(3)$, $c = 11.8158(5)$ and $11.7988(4)$, respectively. In both samples low-occupied $T1$ and $T2$ sites are populated by minor B and Al, which agrees with their high-temperature origin. According to our experimental results, the general revised crystal-chemical formula of vesuvianite can be written as $^{VII-IX}X_{19}\,^V Y_1\,^{VI}Y_{12}(Z_2O_7)_4(ZO_4)_{10}(W)_{10}$, where X are seven-to nine-coordinated sites of Ca with minor Na, K, Fe^{2+} and *REE* impurities; $^V Y$ has a square pyramidal coordination and is occupied predominantly by Fe^{3+} with subordinate Mg, Al, Fe^{2+} and Cu^{2+}; ^{VI}Y has octahedral coordination and is predominantly occupied by Al with subordinate Mg, Fe^{2+}, Fe^{3+}, Mn^{2+}, Mn^{3+}, Ti, Cr and Zn; $ZO_4 = SiO_4$, sometimes with subordinate AlO_4 and/or $(OH)_4$, and $W = OH$, F, with minor O and Cl. The idealized charge-balanced formula of the vesuvianite end-member without subordinate cations is $Ca_{19}Fe^{3+}(Al_{10}Me^{2+}{}_2)(Si_2O_7)_4(SiO_4)_{10}O(OH)_9$, where $Me = Fe^{2+}$, Mg^{2+}, Mn^{2+}.

1. Introduction

The vesuvianite-group minerals are widespread in different contact rocks (including skarns formed during contact or regional metamorphism of limestones; in garnetized gabbros, mafic and ultramafic rocks, and serpentinites) of metamorphic, volcanic and hydrothermal origin [1]. They crystallize in

a wide range of *PT* conditions (0–8 kbar and 200–800 °C) at the greenschist up to granulite facies of metamorphism and can be considered as a geothermometer [2]. Because of their crystal structure flexibility, vesuvianite-group minerals can contain variable amounts of di- and trivalent cations, and they are stable under reducing and oxidizing conditions [3].

First found by Kappeler [4] at the Somma-Vesuvius volcanic complex, vesuvianite was initially confused with garnets, schorl, and even obsidian [5]. It was established later as a mineral species with its present name by Werner [6]. Many authors tried to determine its formula on the basis of the chemical data [7–10], but only structural investigations made it possible to propose the first rational formula for vesuvianite, $Ca_{10}Al_4(Mg,Fe)_2Si_9O_{34}(OH)_4$ [11]. Another formula provided by Machatschki [12] is $X_{19}Y_{13}Z_{18}(O,OH)_{76}$, where X = Ca (partly with minor Na, K, Mn), Y = Al, Fe^{3+}, Fe^{2+}, Mg, Ti, Zn, Mn, and Z = Si, which is comparable with the improved formula, $Ca_{19}(Mg,Fe,Al,Ti,Mn)_5Al_8(O,OH)_{10}(SiO_4)_{10}(Si_2O_7)_4$ [13], determined on the basis of accurate single-crystal XRD studies. Boron incorporation into additional *T* sites (*T*1 with tetrahedral coordination and *T*2 with triangular coordination) of the vesuvianite structure is reflected in the following formula: $X_{19}Y_{13}Z_{18}T_{0-5}O_{68}W_{10}$ [14], where X = Ca, Na, REE^{3+}, Pb^{2+} and Sb^{3+}; Y = Al, Mg, Fe^{3+}, Fe^{2+}, Ti^{4+}, Mn, Cu and Zn; Z = Si; T = B; W = (OH, F, O). Over the past 50 years, numerous substitution schemes have been established that significantly expand the crystal-chemical diversity of the vesuvianite group:

$$^{T1}B^{3+} + {}^{Y}Mg^{2+} + 2^{O10,11}O^{2-} \leftrightarrow {}^{T1}\square + {}^{Y}Al^{3+} + 2^{O10,11}(OH)^- \text{ and } {}^{T2}B^{3+} + 2^{O10,11}O^{2-} \leftrightarrow {}^{T2}\square + {}^{O10,11}(OH)^- \text{ in wiluite [15]}$$

$$^{Y1}Mn^{3+} \leftrightarrow {}^{Y1}Fe^{3+} \text{ in manganvesuvianite [16]}$$

$$^{Z1,2}(SiO_4)^{4-} \leftrightarrow {}^{Z1,2}(H_4O_4)^{4-} \text{ [17]}$$

$$^{O10}OH^- + {}^{O11}OH^- \leftrightarrow {}^{O10}F^- + {}^{O11}F^- \text{ in fluorvesuvianite [18]}$$

$$^{O10}OH^- \leftrightarrow {}^{O10}Cl^- \text{ [19]}$$

$$^{X3}Bi^{3+} + {}^{Y2,3}Mg^{2+} \leftrightarrow {}^{X3}Ca^{2+} + {}^{Y2,3}Al^{3+} \text{ [20]}$$

$$^{Y2}Mg^{2+} + {}^{Y3}Ti^{4+} \leftrightarrow {}^{Y2}Al^{3+} + {}^{Y3}Al^{3+} \text{ [21]}$$

$$^{X1,4}Ca^{2+} + {}^{Y2,3}Al^{3+} \leftrightarrow {}^{X1,4}Na^+ + {}^{Y2,3}Ti^{4+} \text{ in "natrovesuvianite" [22]}$$

$$^{Y1}Cu^{2+} + {}^{Y2,3}Mn^{3+} \leftrightarrow {}^{Y1}Fe^{3+} + {}^{Y2,3}Mg^{2+} \text{ in cyprine [23]}$$

$$^{Y1}Mg^{2+} + {}^{Y3}Al^{3+} \leftrightarrow {}^{Y1}Fe^{3+} + {}^{Y3}Mg^{2+} \text{ in magnesiovesuvianite [24]}$$

$$^{Y1}Fe^{3+} \leftrightarrow {}^{Y1}Al^{3+} \text{ in alumovesuvianite [25]}$$

At present, the vesuvianite group consists of seven mineral species (Table 1), distinguished by the dominant component at five-coordinated *Y*1 site, as well as *T*1 and *T*2 and anionic *W* positions. Taking into account cation ordering in the octahedral positions and the incorporation of additional B, Na and $(H_4O_4)^{4-}$ into the structure, the general formula of the vesuvianite-group minerals can be written as follows (Z = 2): $X_{16}X1_2X4Y1Y2_4Y3_8T_{0-5}(Z_2O_7)_4[(ZO_4)_{10-x}(H_4O_4)_x](W)_9O_{1-3}$, where $x < 3$, X are seven- to nine-coordinated sites (Ca, Na, K, Fe^{2+}, *REE*), *X*4 has square antiprismatic coordination (Ca, Na), *Y*1 has square pyramidal coordination (Fe^{3+}, Mg, Al, Fe^{2+}, Cu^{2+}), *Y*2 and *Y*3 have octahedral coordination (Al, Mg, Zn, Fe^{2+}, Fe^{3+}, Mn^{2+}, Mn^{3+}, Ti, Cr, Zn), *T* is the additional site with triangular or tetrahedral coordination (B, Fe), ZO_4 [SiO_4, $\square$, $(OH)_4$, AlO_4] and Z_2O_7 (Si_2O_7) and the additional anionic position *W* can be occupied by OH, F, or minor O, Cl [12,13,15,17,19,21,26–29].

The crystal structure of vesuvianite-group minerals contains half-populated cation sites arranged along the fourfold axis in the *Y*1–*X*4–*X*4–*Y*1 sequence with the *Y*1–*X*4 and *X*4–*X*4 distances less than 1.3 Å and 2.5 Å, respectively [28]. Cation ordering at the *Y*1 and *X*4 sites produces different ordering schemes and leads to the lower symmetry $P4/nnc \rightarrow P4/n$ and $P4/nnc \rightarrow P4nc$ [13,30], which results in the appearance of subsites (for example *Y*1A and *Y*1B instead *Y*1, *X*4A and *X*4B instead *X*4, etc.).

Table 1. Dominant components in crystallographic sites of vesuvianite-group minerals [1].

Mineral/Formula	*X1, X2, X3*	*X4*	*Y1*	*Y2*	*Y3*	*T1*	*T2*	O10	O11	O12	Reference
Vesuvianite *s.s.*	Ca	Ca	Fe^{3+}	Al	Al	□	□	OH	OH	□	[30]
Fluorvesuvianite	Ca	Ca	Fe^{2+}	Al	Al	□	□	F	F	□	[18]
Manganvesuvianite	Ca	Ca	Mn^{3+}	Al	Al	□	□	OH	OH	□	[16]
Cyprine	Ca	Ca	Cu	Al	Al	□	□	OH	OH	□	[23]
Magnesiovesuvianite	Ca	Ca	Mg	Al	Al	□	□	OH	OH	□	[24]
Alumovesuvianite	Ca	Ca	Al	Al	Al	□	□	OH	OH	□	[25]
Wiluite	Ca	Ca	Mg	Al	Al	B	B	O	O	O	[14,29]
Hongheite	Ca	Ca	Fe^{2+}	Al	Fe^{3+}	□	B	O	O	□	[31]

[1] Vesuvianite-group minerals are characterized by domain structure, and their symmetry is connected with the kind of cation ordering along the four-fold axis [space groups are either tetragonal (*P*4/*nnc*, *P*4/*n*, *P*4*nc*, or *P*-4) or monoclinic (*P*2/*n* or *Pn*)] [12,32–34]. Some crystals contain growth sectors showing triclinic distortion [35].

However, the general formula of vesuvianite given in the International Mineralogical Association (IMA) List of Minerals (http://ima-cnmnc.nrm.se/imalist.htm), $(Ca,Na)_{19}(Al,Mg,Fe)_{13}(SiO_4)_{10}(Si_2O_7)_4(OH,F,O)_{10}$ [36], does not explicitly show the occupancies of the *Y*1 site. This simplified formula is now out of date since it refers to five vesuvianite-group minerals: vesuvianite *sensu stricto*, manganvesuvianite, cyprine, magnesiovesuvianite and alumovesuvianite. For this reason, we report the results of a multimethodological study of two vesuvianite samples from the type locality of this mineral, i.e., the Somma-Vesuvius complex, Campania, Italy. The studied samples nos. **27844** and **51062** originate from the Vesuvius collection of the Fersman Mineralogical Museum, Moscow. The aim of this work is to establish a correct formula of vesuvianite, which does not contradict the IMA Commission on New Minerals, Nomenclature and Classification (CNMNC) guidelines [37].

2. Occurrence

Vesuvianite from the Somma-Vesuvius volcanic complex (Campania region, Southern Italy), typically occurs in various kinds of xenolithic rocks, commonly associated with various Plinian eruptives and found as ejecta in pyroclastic deposits [38–41].

The typical occurrence of vesuvianite is related to xenoliths of skarn, a largely mineralogically zoned, coarse-grained Ca-Mg-Fe(Mn)-rich silicate rocks [42]. At Somma-Vesuvius, these rocks are very complex in mineralogical and textural aspects. Most of skarns at Somma-Vesuvius complex show a sequence of mono- or bimineral zones dominated by Ca- and/or Mg-silicates, such as clinopyroxene, phlogopite, wollastonite, meionite, olivine, or clinohumite, and other minerals (perovskite, spinel, calcite, etc.) commonly with a central cavity containing euhedral crystals of vesuvianite, garnet, wollastonite, gehlenite, or anorthite. Mono- or bimineral skarns, as well as composite ejecta (consisting of two or more rock types, such as skarn-marble, skarn-hornfels, cumulate-skarn or cumulate skarn-marble are common and document the close spatial association of at least some of these rock types at depth) with sharp contacts of skarns to marbles or hornfelses are common [42–44]. The mineralogical composition of skarn ejecta generally includes highly variable amounts of vesuvianite, wollastonite, clinopyroxene (diopside, hedenbergite, low-iron augite, i.e., "*fassaite*"), anorthite, phlogopite, clinoamphibole, garnet (mainly of the grossular-andradite series), forsterite, and humite-group minerals. Other minerals locally observed as minor to accessory phases include melilite (gehlenite), feldspathoids (leucite, nepheline, sodalite, haüyne, nosean, scapolite, meionite, davyne, balliranoite), fluorapatite, fluorite, cuspidine, zircon, perovskite, calcite, baddeleyite, spinels (spinel *sensu stricto*, magnetite), *REE*-minerals, sulfides, etc. [41,42]. The vesuvianite-bearing calc-silicate ejecta are most likely related to the Plinian eruptions of *Avellino* (3800 BC) and *Pompeii* (79 AD) [44]. The investigations of fluid inclusions as well as the isotope compositions of Pb, Nd and Sr have been carried out, among others, on vesuvianite crystals as reported in [42]. According to [42], the formation of skarns can be related to assimilation of carbonate-wall rocks by the alkaline magma at moderate depths (<5 km), and consequent exsolution of CO_2-rich vapor and complex saline melts from the contaminated magma that reacted with the carbonate rocks to form

skarns. According to fluid inclusion studies [42], the estimated temperature of the formation skarn minerals at Somma-Vesuvius complex is in the range 800–900 °C.

Together with the skarn occurrence, vesuvianite has been also observed in thermally metamorphosed carbonate nodules ("marbles" [5]), interpreted as the result of recrystallization and in part, devolatilization without significant metasomatic interaction with aqueous fluids or silicate melts [42]. In these calcitic marbles, vesuvianite is variably associated with (i) wollastonite, clinopyroxene, sodalite and humite; (ii) clinopyroxene, sodalite, cuspidine, forsterite, nepheline and davyne; or (iii) sanidine, fluorite, fluorapatite and sulfides [5].

In addition, vesuvianite occurs as an accessory mineral in syenitic K-feldspar-rich nodules [5,39]. In this rock, it is locally observed in vugs and cavities as grains (<1 mm) among the tabular sanidine crystals, in association with garnet, clinoamphibole, clinopyroxene, davyne, titanite, or with fluorite, zircon and wöhlerite-group minerals [5]. In [39], accessory vesuvianite crystals (~200–500 μm) were observed in the K-feldspar syenitic ejecta together with other minor to trace phases that can be alternatively represented by clinoamphibole, clinopyroxene, biotite, plagioclase, sodalite, nosean, nepheline, hematite, magnetite, fluorite and titanite. Vesuvianite also occurs in sanidinite ejecta found at the San Sebastiano valley at Vesuvius in association with pyrochlore, magnetite, wöhlerite group minerals, baddeleyite, zircon, fluorite, ferrohornblende, phlogopite and nepheline [45].

In samples **51062** and **27844** (Figure 1), euhedral vesuvianite occurs in association with grossular and clinozoisite or as a monomineralic aggregate, respectively; the large sizes of the crystals indicate their skarn provenance. In particular, the association of vesuvianite with garnet, wollastonite, gehlenite or anorthite in the first sample is typical for zoned skarns of the Somma-Vesuvius complex [42]. It is worth nothing that the occurrence of clinozoisite in the sample **51062** represents, to the authors' knowledge, the first record of this mineral at Somma-Vesuvius.
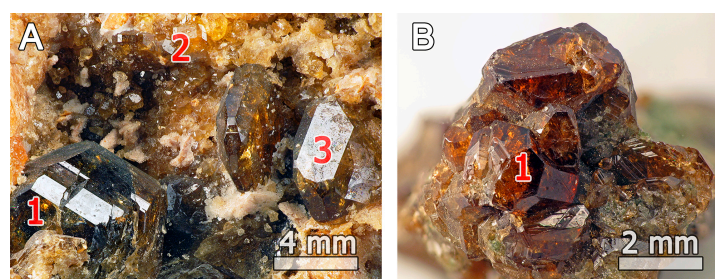

Figure 1. Short-prismatic vesuvianite crystals (1) associated with grossular (2), and clinozoisite (3), in samples (**A**) **51062** and (**B**) **27844**.

3. Materials and Methods

Both vesuvianite samples studied in this work (**27844** and **51062**) form well-shaped short-prismatic crystals up to 6 mm long (Figure 1) with the main prismatic forms {100} and {110} terminated by the pyramidal {101} and pinacoidal {001} faces. The crystals are lustrous and semi-transparent. Their color varies from greenish brown (**27844**) to brownish green and orange-brown in the marginal zone (**51062**).

Chemical analyses of both samples (Table 2, each analysis is the mean from 4 to 7 points) were obtained using a HITACHI S-3400N scanning electron microscope (Tokyo, Japan) equipped with INCA Wave 500 WDS spectrometer. The system was operated at 20 kV and 10 nA, and the electron beam was focused to a 5 μm spot. The following standards were used: rutile (Ti), wollastonite (Si, Ca), forsterite (Mg), fluorite (F), cryolite (Na), halite (Cl), spessartine (Mn, Al), hematite (Fe), danburite (B), synthetic Ce-glass (Ce), synthetic Nd-glass (Nd). The content of boron was measured at the Faculty of Geology, University of Warsaw, by a CAMECA SX100 instrument operated at 6 kV and 80 nA for 50–100 s counting at each point (Kα line, PC2 crystal (Ni/C-LSM), standard deviation 0.25 wt % B_2O_3). No other elements having atomic numbers above eight were found above their detection limits. The content of H_2O in **27844** was determined by means of thermogravimetric analysis using NETZSCH STA 449 F3

Jupiter thermoanalyzer (Exton, PA, USA) during 10 °C/min heating of a 68.4 mg sample from room temperature to 1100 °C in a dynamic argon atmosphere, with aluminum oxide standard.

Table 2. Single-crystal data, data collection and structure refinement parameters.

Sample	27844	51062
Temperature/K	293(2)	293(3)
Crystal system	Tetragonal	Tetragonal
Space group	$P4/nnc$	$P4/nnc$
$a = b$ (Å)	15.5720(3)	15.5459(3)
c (Å)	11.8158(5)	11.7988(4)
Volume (Å^3)	2865.16(16)	2851.48(16)
Z	2	2
ρ_{calc} (g/cm^{-3})	3.395	3.405
μ (mm^{-1})	2.839	2.837
$F(000)$	2941.0	2901.0
Crystal size (mm^3)	$0.21 \times 0.15 \times 0.14$	$0.22 \times 0.19 \times 0.17$
Radiation	MoKα (λ = 0.71073)	MoKα (λ = 0.71073)
2θ range for data collection (°)	5.232–54.982	6.802–54.974
Index ranges	$-20 \leq h \leq 19$ $-15 \leq k \leq 20$ $-15 \leq l \leq 14$	$-13 \leq h \leq 20$ $-14 \leq k \leq 15$ $-15 \leq l \leq 7$
Reflections collected	14,428	5687
Independent reflections	1653 [R_{int} = 0.0440 R_{sigma} = 0.0178]	1622 [R_{int} = 0.0274 R_{sigma} = 0.0267]
Data/restraints/parameters	1653/0/162	1622/0/162
Goodness of fit on F^2	1.184	1.114
Final R indices [$I > 2\sigma(I)$]	R_1 = 0.027 wR_2 = 0.072	R_1 = 0.030 wR_2 = 0.078
Final R indices [all data]	R_1 = 0.028 wR_2 = 0.072	R_1 = 0.035 wR_2 = 0.080
Largest diff. peak/hole (e Å^{-3})	0.56/−1.05	0.53/−1.08

The ^{27}Al nuclear magnetic resonance (NMR) spectrum was obtained at room temperature by means of a Bruker Avance III 400 WB spectrometer (Billerica, MA, USA) at 104.24 MHz. The magic-angle spinning (MAS) spin rate of the rotor was 20 kHz. For these investigations, a single-pulse sequence with a pulse length of 86 kHz was used, with the recycle delay of 1 s and 4096 scans. The 1H NMR spectrum was obtained at room temperature using a Bruker Advance III 400 WB spectrometer operating at 400.23 MHz. The MAS spin rate of rotor was 20 kHz. A single-pulse sequence was used with a pulse length of 100 kHz, recycle delay of 20 s and 32 scans.

The Fe^{2+}/Fe^{3+} ratio is given in accordance with the Mössbauer spectrometry data. Gamma-resonance studies of **27844** and **51062** were carried out using a commercial Mössbauer spectrometer (WissEl Wissenschaftliche Elektronik GmbH, Starnberg, Germany) in order to clarify the valence state of iron and the coordination environment(s) of the Fe. The spectrometer was equipped with a standard radioactive source, ^{57}Co, in a rhodium matrix (Ritverc). The absorption-mode measurements have been performed at room temperature. The samples were crushed in an agate mortar, distributed homogeneously within the punch-holder and packed in the form of a tablet with a density of 112 mg/cm^2 in order to optimize the conditions for measurement. The spectral fitting of the experimental Mössbauer spectrum was carried out by the method of least squares under the assumption of Lorentz-shaped spectral lines. Isomer shifts were measured relative to metallic iron. The mathematical analysis was performed with the commercial Mössbauer software SpectRelax Version 2.1 (Moscow State University, Moscow, Russia).

A FTIR spectrum of **27844** was collected using a Bruker ALPHA spectrometer at room temperature in the range 360–3800 cm^{-1} (KBr pellet, resolution 4 cm^{-1}, 16 scans). A pure KBr pellet was used as a reference.

Powder X-ray diffraction data (Table A1) were collected with a Bruker Phaser D2 diffractometer in the 2θ range of 10–80° (CuKα; 1.5418 Å), with a scanning step of 0.02° (1 s per step) in 2θ.

Single-crystal X-ray diffraction experiments were carried out using an Agilent Technologies Xcalibur Eos diffractometer (Agilent Technologies, Santa Clara, CA, USA) operated at 50 kV and 40 mA. A hemisphere of three-dimensional data was collected at 293 K for each sample using monochromatic Mo *K*α radiation, with frame widths of 1° and 20 s count for each frame. The crystal-to-detector distance was 45 mm. For the investigated samples, *P*4/*nnc* was chosen as the most probable space group. Only 79 reflections violating the absence conditions in the range 2σ(*I*) < *I* < 188σ(*I*) with maximum F_o^2 = 881 were found for **27844**, whereas only 15 such reflections with 2σ(*I*) < *I* < 382σ(*I*) and maximum F_o^2 = 2021 were observed for **51062**. Refinements of both structures in space groups *P*4/*n* and *P*4*nc* did not indicate any reasons for the symmetry lowering from the *P*4/*nnc* space group.

The crystal structures of **27844** and **51062** were refined to R_1 = 0.027 and R_1 = 0.035 for 1653 and 1622 unique observed reflections with $|F_o| \geq 4\sigma F$, respectively, using the SHELX program [46]. Empirical absorption corrections were applied in the CrysAlisPro program complex [47] using spherical harmonics, implemented in the SCALE3 ABSPACK scaling algorithm. The final difference Fourier map showed no features higher than 0.53/0.56 *e*$^-$ for **27844** and **51062**, respectively. The experimental details and crystallographic parameters are given in Table 2. Crystallographic information files (CIFs) are deposited in the electronic Supplementary Materials.

4. Results

4.1. Chemical Composition

The crystal-chemical formulae of the investigated samples (Table 3) were calculated on the basis of 19 *X*-cations (Ca + Na + *REE*). Both compositions are in good agreement with the previous data for vesuvianite from the Monte-Somma-Vesuvius complex [38,48].

Table 3. Chemical composition of **27844** and **51062** [1].

Component	wt %		Component	*apfu*	
	27844	51062		27844	51062
SiO$_2$	36.41	35.89	Si	17.81	17.99
Al$_2$O$_3$	15.82	15.93	Al	9.12	9.41
TiO$_2$	bd	0.41	Ti	bd	0.16
Fe$_2$O$_3$ [1]	3.48	2.97	Fe^{3+}	1.28	1.12
FeO [1]	0.98	1.29	Fe^{2+}	0.40	0.54
MnO	0.27	0.38	Mn	0.11	0.16
MgO	2.51	3.21	Mg	1.83	2.40
CaO	36.19	35.19	Ca	18.97	18.90
Ce$_2$O$_3$	bd	0.33	Ce	bd	0.06
Nd$_2$O$_3$	bd	0.22	Nd	bd	0.04
Na$_2$O	0.03	bd	Na	0.03	bd
B$_2$O$_3$ [2]	0.83	0.79	B	0.70	0.68
Cl	0.06	0.05	Cl	0.05	0.04
F	1.29	1.22	F	2.00	1.93
H$_2$O [3]	1.60	1.76	OH	5.22	5.88
–O=F,Cl	−0.56	−0.52	O	73.04	74.75
Total	98.90	98.57			

[1] Although Fe was measured as Fe$_2$O$_3$, it is reported as Fe$_2$O$_3$ and FeO based on the results from Mössbauer spectroscopy data; [2] Boron content measured using a CAMECA SX-100 instrument at the same grains (PC2 crystal, 6 kV and 80 nA for 50–100 s at each point, mean of 7 point analyses); [3] The content of H$_2$O measured by thermogravimetry (TGA) method for **27844** and calculated from the structural data for **51062**.

4.2. Thermogravimetric Analysis and Differential Scanning Calorimetry (TGA/DSC)

The TGA curve (Figure 2) of **27844** contains one major step of weight loss, accompanied by two endothermic effects at 980 °C and 1030 °C in the DSC-curve, which can be assigned to separated dehydroxylation processes for the O(11)H and O(10)H groups [23,49]. According to [49,50] one-step weight loss in the temperature range of 820–1090 °C is characteristic for low-temperature vesuvianite. Weight loss in the range of 990–1150 °C responds to the high-symmetry vesuvianite. The total weight loss for **27844** is 1.60 wt %, which corresponds to 5.22 OH-groups per formula unit. As a result of dehydroxylation, vesuvianite transforms into the mixture of wollastonite, grossular, quartz and an amorphous glass-like substance.
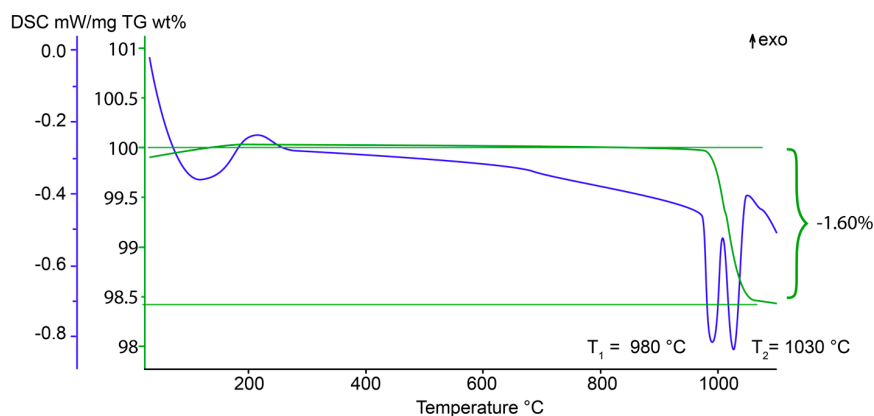
Figure 2. Thermogravimetric (wt %, green line) and differential scanning calorimetry (blue line) curves for **27844**.

4.3. Solid State Magic-Angle Spinning Nuclear Magnetic Resonance (MAS NMR)

The ^{27}Al MAS NMR spectrum (Figure 3) of **27844** contains one broad peak, which is centered at −2.5 ppm and can be assigned to the octahedrally coordinated Al at the *Y*2 and *Y*3 sites [41–52]. Similarly to wiluite, broadening of the peak at 60 ppm can be assigned to a trace amount of Al in the 4-coordinated *T*1 site (<1 *apfu*) [29]. The weak symmetric peaks observed near ±190 ppm belong to spinning sidebands.

The ^{1}H MAS NMR spectrum (Figure 3) of **27844** contains two peaks centered at 6.9 and 1.5 ppm, respectively. Calculations of the O···O distances using the equation $\delta_{iso}(ppm) = 79.05 - 0.255d$ (O–H···O)(pm) [53] provided the values of 2.83 Å and 3.04 Å. The most intense peak at 6.9 ppm corresponds to the O11–H1a···O7 and O10–H2···O10 hydrogen interactions, which is in agreement with the distances 2.784(4) and 2.74–2.82 Å reported by other authors [54–59]. A low intense line at 1.5 ppm can be assigned to the H1b site, since its chemical shift agrees well with the O11–H1···O11 distances of 3.01–3.04 Å [54,57].
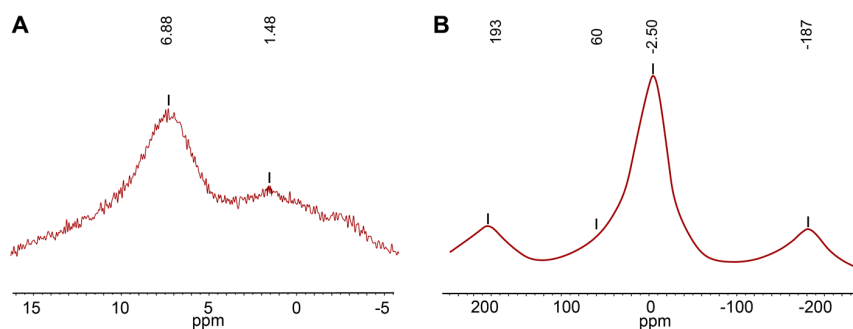

Figure 3. (**A**) ^{1}H MAS NMR and (**B**) ^{27}Al MAS NMR spectra of **27844**.

4.4. Mössbauer Measurenments

The Mössbauer spectra of **27844** and **51062** can be described as a superposition of five and four symmetric doublets, respectively (Figure 4). The assignments based on the crystal-structure refinement and Mössbauer parameters of these doublets (isomer shifts *IS*, quadrupole splittings *QS*, line widths and areas under resonance doublets *S*) according to [21,60,61] are listed in Table 4. Trivalent iron dominates in both samples: *C* doublets with *IS* = 0.38, 0.38, *QS* = 0.49, 0.52 and *S* = 54, 60% are assigned to Fe^{3+} at *Y*3 octahedra, whereas *E* doublet with *IS* = 0.48, 0.41, *QS* = 1.08, 1.31 and *S* = 12.8, 16.3 corresponds to Fe^{3+} at the five-coordinated *Y*1 site. *D* doublets with *IS* = 0.82, 0.84, *QS* = 0.40, 0.43 and *S* = 18, 15% correspond to divalent iron at the octahedral *Y*3 site. The *B* doublets with *IS* = 1.02, 1.03, *QS* = 2.92, 2.92 and *S* = 18, 15%, similar to doublets reported in [21,61–63], correspond to minor amounts of Fe^{2+} at the *Y*1 site. The *G* doublet with *IS* = 0.92 and *QS* = 2.40 observed in the Mössbauer spectra of **27844** and wiluite [29] can be assigned to the octahedrally coordinated Fe^{2+} incorporated into the *Y*2 site.

Table 4. Parameters of the Mössbauer spectra of **27844** and **51062** at 293 K.

Designation of the Quadrupole Doublet	Isomer Shift (mm/s)	Quadrupole Splitting (mm/s)	Line Width (mm/s)	Relative Area (%)	Assignment [1]
Sample			27844		
C	0.377 ± 0.002	0.492 ± 0.004		54.4 ± 0.6	$^{VI}Fe^{3+}$ in *Y*3
E	0.481 ± 0.006	1.076 ± 0.011		12.8 ± 0.7	$^{V}Fe^{3+}$ in *Y*1
D	0.821 ± 0.003	0.396 ± 0.004	0.460 ± 0.004	17.9 ± 0.5	$^{VI}Fe^{2+}$ in *Y*3
B	1.039 ± 0.012	2.920 ± 0.031		6.1 ± 0.5	$^{V}Fe^{2+}$ in *Y*1
G	0.921 ± 0.009	2.400 ± 0.022		8.8 ± 0.5	$^{VI}Fe^{2+}$ in *Y*2
Sample			51062		
C	0.377 ± 0.007	0.528 ± 0.014		59.9 ± 0.4	$^{VI}Fe^{3+}$ in *Y*3
E	0.405 ± 0.004	1.312 ± 0.010	0.432 ± 0.004	16.3 ± 0.5	$^{V}Fe^{3+}$ in *Y*1
D	0.842 ± 0.030	0.438 ± 0.060		14.8 ± 0.4	$^{VI}Fe^{2+}$ in *Y*3
B	1.030 ± 0.007	2.920 ± 0.014		9.0 ± 0.3	$^{V}Fe^{2+}$ in *Y*1

[1] The symbols and the assignment of the quadrupole doublets are given in accordance with the data from [21,29,61] based on the analysis of Mössbauer spectra of 17 vesuvianite samples from different localities. Taking into account Fe–O distances and site multiplicities, quadrupole doublet *d* with anomalously low quadrupole splitting could not be assigned to Fe at distorted *Y*1 sites.
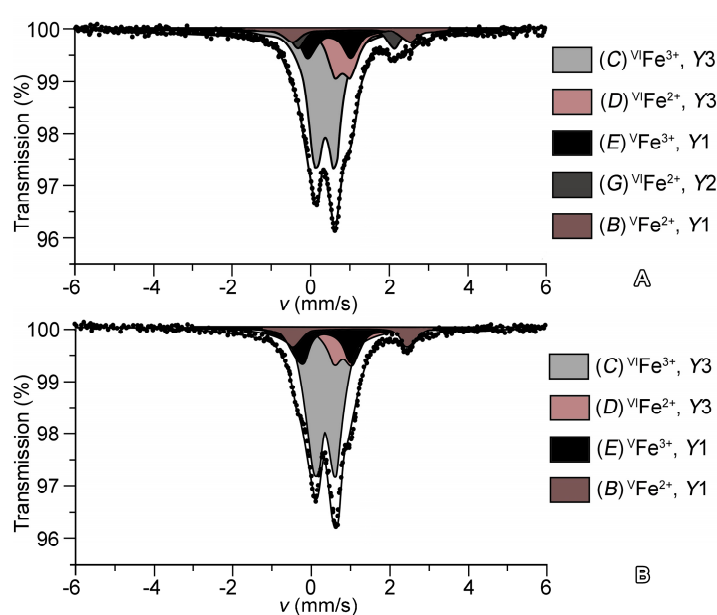

Figure 4. Mössbauer spectra of (**A**) **27844** and (**B**) **51062**.

4.5. X-ray Crystallography

The unit-cell dimensions of **27844** were determined from the X-ray powder-diffraction pattern (Figure 5) by Rietveld refinement using the program Topas 4.2 [64] and are in a good agreement with the single-crystal XRD data: a = 15.5779(6) Å, c = 11.8156(6) Å, V = 2867.3(4) Å^3.
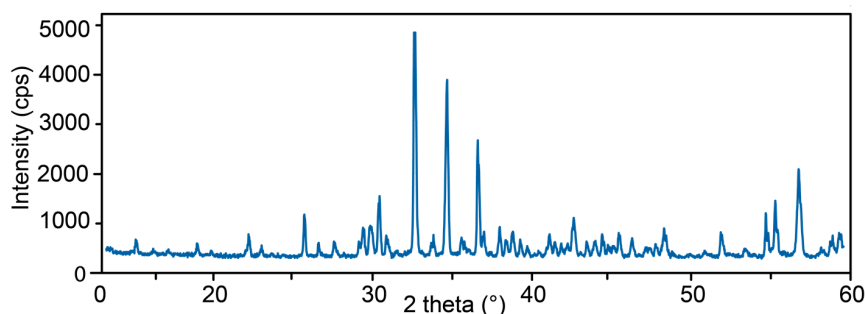

Figure 5. Powder diffraction pattern of **27844**. All reflections refer to vesuvianite (Table A1).

Structural models of **27844** and **51062** are close to that reported in [48], with site designations according to [15]. We pay particular attention to the occupancy of the *Y1* site that plays a key role in the diversity of the vesuvianite-group minerals.

In the crystal structure of vesuvianite, the five-coordinated *Y1* site (Table 1 and Figure 6) can be occupied by Fe^{3+}, Fe^{2+}, Mn^{3+}, Mn^{2+}, Cu, Mg and Al [16,23,30,51,52,55,65]. In most cases, including previously studied vesuvianite from the Somma-Vesuvius volcanic complex, Fe^{3+} dominates in the *Y1* site [48]. In accordance with the ^{27}Al MAS NMR data, five-coordinated Al^{3+} in **27844** is absent, and the final occupancy of the *Y1* site is determined by Fe and Mg. In the structures of **27844** and **51062**, iron is predominant at the *Y1* site: $(Fe_{0.72}Mg_{0.28})_{1.00}$ and $(Fe_{0.73}Mg_{0.27})$, respectively, or, taking into account Mössbauer data, $Fe^{3+}_{0.50}Mg_{0.28}Fe^{2+}_{0.22}$ and $Fe^{3+}_{0.47}Mg_{0.27}Fe^{2+}_{0.26}$, respectively. Scattering of the *Y2* site in both samples is close to 13 $\bar{e}$, and the average <*Y2*–O> bond lengths are equal to 1.896 and 1.895 Å for **27844** and **51062**, respectively, which agrees well with the site occupancy by Al atoms only. The octahedral *Y3* site has minor admixtures of iron (mainly Fe^{3+}), which is confirmed by a slightly higher mean length of the <*Y3*–O> bonds: 1.966 and 1.961 Å, respectively. The total refined *Y3* site occupancies are $(Al_{0.90}Fe_{0.10})_{1.00}$ and $(Al_{0.91}Fe_{0.09})$, respectively. Both the contents and oxidation states of iron have been confirmed by the Mössbauer data.
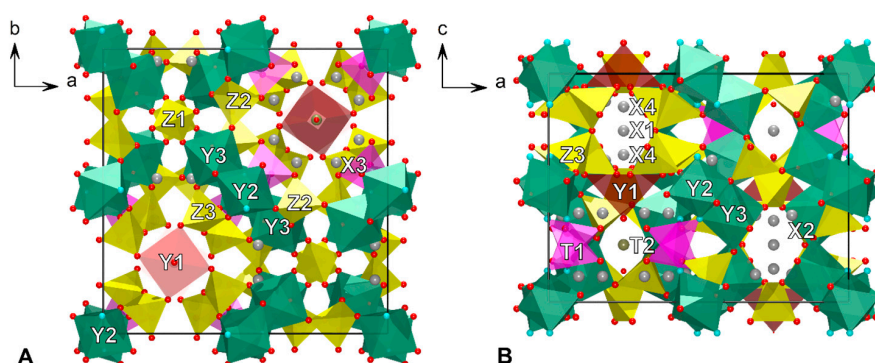

Figure 6. The crystal structure of **27844** projected along (**A**) *c* axis and (**B**) *b* axis. *T*-sites have low occupation: *T1* ≈ 10% and *T2* ≈ 25%. The O11 site with mixed $(O_{0.75}F_{0.25})$ occupancy represent by blue circles, oxygen atoms are red circles.

The mean <*Z* − O> bond lengths and scattering factors of the tetrahedral *Z1*, *Z2* and *Z3* sites are in agreement with the full occupancies of these sites by Si atoms only.

In the refinement model, the 7- to 9-coordinated *X1*, *X2*, *X3* and *X4* sites are completely populated by Ca. The *X* sites have full occupancies except for the eightfold-coordinated *X4* position that is half-populated and is situated in the structure channels. According to [66], *REEs* incorporate into the *X3* site, but their low content (1.5% of the *X3* site occupancy) cannot be precisely determined by the structural analysis. Similar reasoning applies also to the admixture of Na in the *X4* site [22].

Incorporation of small amounts of boron into the vesuvianite structure does not lead to the splitting of the O7 site and the appearance of the O12 site as it does in wiluite [67]. The low-occupied *T2* site (Figure 7) is populated by about 25% boron, which prevented us from the determination of its coordination. However, the presence of 3-coordinated boron is confirmed by FTIR. The observed scattering factors of the *T1* site of 1.4 and 1.0 e^- correspond to the refined occupancies $Al_{0.106}$ and $Al_{0.072}$, respectively. Due to the low occupancies of the *T1* site, the mean <*T1*–O> bond lengths, 1.827 and 1.830 Å, are significantly longer than the theoretical one for tetrahedrally coordinated Al with full occupancy. At the same time, the presence of small amounts (~0.45 *apfu*) of tetrahedrally coordinated boron at the *T1* site cannot be excluded.

All oxygen sites have been refined as fully occupied by oxygen atoms, excluding the O7 site that possesses anomalously high displacement parameters. In the final model, the O7 site was refined as $(O_{0.75}F_{0.25})_{1.00}$ with plausible displacement parameters. Small amounts of Cl determined by the electron microprobe (0.05 and 0.04 *apfu* for **27844** and **51062**, respectively) are probably situated in the O10 site [19].

Taking into account all of the data given above, the final crystal-chemical formulae of the **27844** and **51062** samples can be written, as follows: $^{X1}(Ca)_{2.00}{}^{X2}(Ca)_{8.00}{}^{X3}(Ca)_{8.00}{}^{X4}(Ca_{0.97}Na_{0.03})_{1.00}$ $^{Y1}(Fe^{3+}{}_{0.50}Mg_{0.28}Fe^{2+}{}_{0.22})_{\Sigma1.00}{}^{Y2}(Al_{3.85}Fe^{2+}{}_{0.15})_{\Sigma4.00}{}^{Y3}(Al_{5.26}Mg_{1.83}Fe^{3+}{}_{0.54}Fe^{2+}{}_{0.26}Mn_{0.11})_{\Sigma8.00}{}^{Z1}(Si)_{2.00}$ $^{Z2}(Si)_{8.00}{}^{Z3}(Si)_{8.00}(O)_{68.00}{}^{T1+T2}(Al_{0.44}B_{0.25}\square_{4.31})_{\Sigma5.00}{}^{W}(OH_{5.65}F_{2.00}O_{1.30}Cl_{0.05})_{\Sigma9.00}$ and $^{X1}(Ca)_{2.00}{}^{X2}(Ca)_{8.00}$ $^{X3}(Ca_{7.90}Ce_{0.06}Nd_{0.04})_{8.00}{}^{X4}(Ca)_{1.00}{}^{Y1}(Fe^{3+}{}_{0.47}Mg_{0.27}Fe^{2+}{}_{0.26})_{\Sigma1.00}{}^{Y2}(Al)_{\Sigma4.00}{}^{Y3}(Al_{5.01}Mg_{2.10}Fe^{3+}{}_{0.53}Fe^{2+}{}_{0.13}$ $Ti_{0.12}Mn_{0.11})_{\Sigma8.00}{}^{Z1}(Si)_{2.00}{}^{Z2}(Si)_{8.00}{}^{Z3}(Si)_{8.00}(O)_{68.00}{}^{T1+T2}(Al_{0.29}B_{0.25}\square_{4.46})_{\Sigma5.00}{}^{W}(OH_{5.88}F_{2.00}O_{1.08}Cl_{0.04})_{\Sigma9.00}$. The Fe content in each *Y* site was assigned according to the crystal-structure data, whereas the Fe^{2+}/Fe^{3+} ratio is given in accordance with the Mössbauer spectroscopy data.
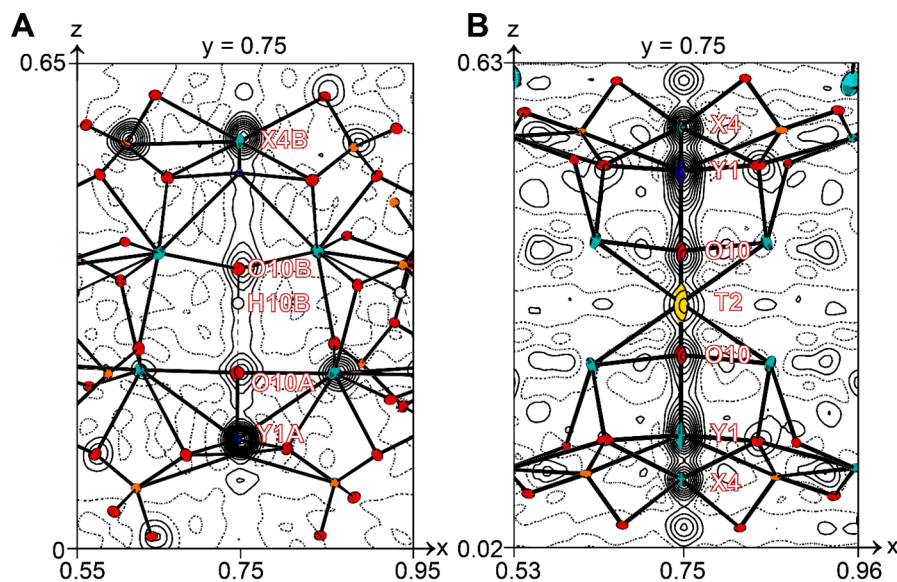

Figure 7. Graphs of observed electron density along the cation rods (fourfold axis is centered at 0.75; 0.75; *z*) in the crystal structures of: (**A**) low-symmetry *P4/n* vesuvianite from Akhmatovskaya Pit and (**B**) **51062**. Projections are onto the (010) plane, contour intervals are 0.1 eÅ^{-3}. Displacement ellipsoids are drawn at the 50% probability level.

4.6. Infrared Spectroscopy

The IR spectrum of **27844** (Figure 8) is typical for high-symmetry vesuvianite-group minerals. It contains strong bands of Si–O stretching in the Si_2O_7 (at 1018 and 976 cm^{-1}) and SiO_4 groups (at 914 cm^{-1} with shoulders at 900 cm^{-1} and 870 cm^{-1}), as well as Si–O–Si and O–Si–O bending vibrations, partly mixed with the *M*–O stretching vibrations, where *M* = Al, Mg, Fe, Ti, Mn (below 700 cm^{-1}). The band at 799 cm^{-1} is assigned to bending vibrations of the *M*···O–H groups.
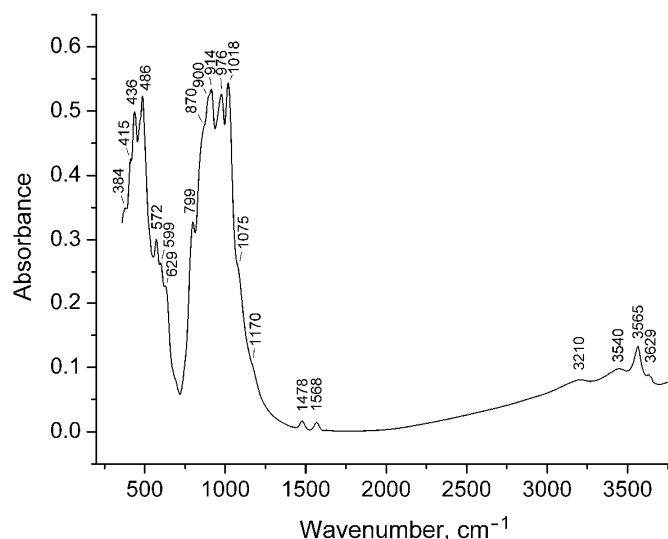
Figure 8. Infrared spectrum of **27844**.

The region of O–H stretching vibrations is dominated by the peak at 3565 cm^{-1} (D band according to [68], which corresponds to the vibrations of the O11–H1 bond in the presence of F in the neighboring O11 site [69]. The weak bands at 3450 cm^{-1} and 3629 cm^{-1} are related to the OH groups coordinated by Ti and to the O11–H1···O7 fragment with the angle <120°, respectively [69]. The weak band at 3210 cm^{-1} (J band) corresponds to the OH groups oriented along the *c*-axis [68] forming strong hydrogen bonds.

Two weak bands at 1568 and 1478 cm^{-1} are assigned to the BO_3^{3-} anions (the *T*2-centered triangle) with shortened (as compared to wiluite) B–O bonds. The shoulders at 1170 cm^{-1} and 1075 cm^{-1} are tentatively assigned to boron atoms having 4-fold coordination.

5. Discussion

Generalization of the vesuvianite formula is an important step for the development of the nomenclature for this group of minerals. The tentative vesuvianite formula, $(Ca,Na)_{19}(Al,Mg,Fe)_{13}(SiO_4)_{10}$ $(Si_2O_7)_4(OH,F,O)_{10}$, does not specify the occupancies of the *Y*1(A,B) site [36], which are responsible for the observed species diversity of the vesuvianite-group minerals [16,21,29]. According to the IMA CNMNC guidelines for compositional criteria [37], at least one structural site in the potential new mineral should be predominantly occupied by a different chemical component than that which occurs in the equivalent site in an existing mineral species [16]. In this context, recently approved members of the vesuvianite group with Mn^{3+}, Al^{3+}, Mg^{2+}, Cu^{2+} as predominant cations at the *Y*1 site can be confused with vesuvianite itself, according to the present formula of this mineral. Therefore, it is crucially important to determine a new vesuvianite formula, which would be in accordance with the above-mentioned IMA rule.

In most cases, vesuvianite with the *P*4/*nnc* symmetry has only Fe and Mg at the *Y*1 site [55]. There are only three publications available that report vesuvianite with the Fe^{2+}/Fe^{3+} ratio determined by direct chemical or spectroscopic methods (Figure 9) [21,29,63]. Our data demonstrate the predominance

of Fe^{3+} at the $Y1$ site for both vesuvianite samples from the type locality, which is consistent with previous conclusions [38,48]. According to our experimental results, the new formula of vesuvianite can be written as $^{VII-IX}X_{19}{}^{V}Y_1{}^{VI}Y_{12}(ZO_7)_4(ZO_4)_{10}(W)_{10}$, where X are seven- to nine-coordinated sites of Ca with minor Na, K, Fe^{2+} and *REE* impurities; ^{V}Y has square pyramidal coordination of dominant Fe^{3+} and subordinate Mg, Al, Fe^{2+} and Cu^{2+}; ^{VI}Y has octahedral coordination and is dominantly occupied by Al with subordinate Mg, Fe^{2+}, Fe^{3+}, Mn^{2+}, Mn^{3+}, Ti, Cr and Zn; $ZO_4 = SiO_4$, sometimes with subordinate AlO_4, $(O_4H_4)^{4-}$, and W = OH, F, Cl and minor O [12,13,15,17,19,21–29]. Since the sum of occupancies of the $T1$ and $T2$ sites is below 1 *apfu*, their populations are not taken into account. The simplified vesuvianite formula may be written as $Ca_{19}Fe^{3+}(Al,Mg,Fe)_{12}(SiO_4)_{10}(Si_2O_7)_4(OH,F,O)_{10}$. The idealized charge-balanced formula of the vesuvianite end-member without subordinate cations is $Ca_{19}Fe^{3+}(Al_{10}Me^{2+}{}_2)(Si_2O_7)_4(SiO_4)_{10}O(OH)_9$, where Me = Fe^{2+}, Mg^{2+}, Mn^{2+}.
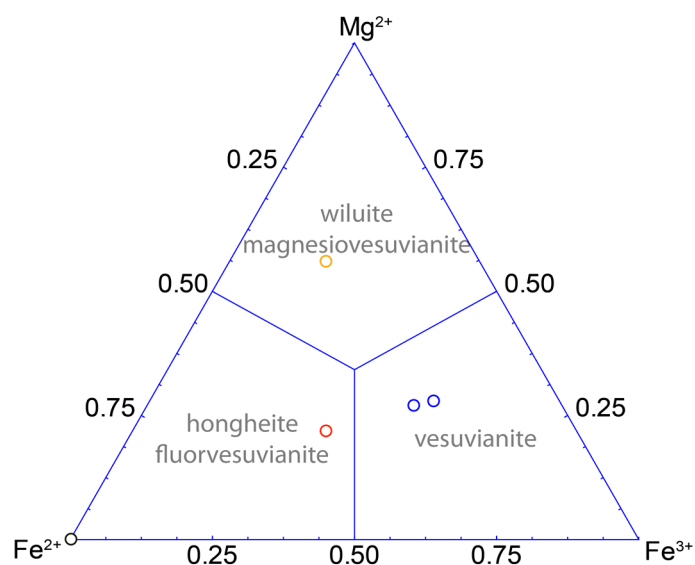

Figure 9. Triangular compositional diagram of the $Y1$ site in the $P4/nnc$ vesuvianite based on single-crystal X-ray diffraction with Fe^{2+}/Fe^{3+} ratio obtained from Mössbauer data [63] (black circle), [21] (red circle), [29] (orange circle) and present study (blue circles)).

6. Conclusions

By revising vesuvianite-group of minerals [16,21,29] two vesuvianite samples **27844** and **51062** from type locality were investigated by electron microprobe analysis, Mössbauer and infrared spectroscopy, TGA/DSC, MAS NMR, single-crystal and powder X-ray diffraction.

Present studies reveal square-pyramidal $Y1$ position as a key site in the diversity of vesuvianite-group minerals. On the basis of this approach we determine vesuvianite formula as $Ca_{19}Fe^{3+}(Al_{10}Me^{2+}{}_2)(Si_2O_7)_4(SiO_4)_{10}O(OH)_9$, which would not contradict present CNMNC guidelines for compositional criteria.

The vesuvianite from the Somma-Vesuvius complex demonstrate disorder inside the structural channels and overall $P4/nnc$ symmetry, which partially connected with the incorporation of boron at additional $T1$, $T2$ sites and agrees with the estimated temperature of crystallization at 800–900 °C.

Appendix A

Table A1. Powder X-ray diffraction data for **27844** [1].

d_{meas} Å	I_{meas}	d_{calc} Å	I_{calc}	hkl	d_{meas} Å	I_{meas}	d_{calc} Å	I_{calc}	hkl
10.83	4	10.84	2	110	2.081	5	2.076	8	623
5.85	4	5.85	2	002	2.060	4	2.060	3	543
4.673	4	4.667	6	202	2.038	9	2.047	13	730
4.000	6	4.027	4	222	2.022	4	2.023	6	642
3.857	2	3.845	2	400	2.008	2	2.001	1	731
3.463	**15**	**3.460**	**15**	**322**	1.9941	8	1.9957	12	633
3.234	4	3.229	6	402	1.9602	6	1.6712	6	651
3.062	5	3.065	5	313	1.9281	2	1.9265	5	116
3.038	8	3.031	6	510	1.9171	2	1.9098	2	713
2.995	9	2.995	14	501	1.9029	4	1.9030	2	206
2.939	**18**	**2.933**	**45**	**511**	1.8823	7	1.8898	11	216
2.897	5	2.895	6	323	1.8647	2	1.8635	2	515
2.744	**100**	**2.748**	**100**	**440**	1.7960	1	1.7950	2	831
2.659	3	2.654	2	530	1.7614	9	1.7587	18	714
2.586	**58**	**2.587**	**60**	**531**	1.7158	2	1.7149	3	910
2.522	6	2.523	5	314	**1.6768**	**17**	**1.6756**	**11**	**734**
2.492	1	2.483	1	611	**1.6603**	**22**	**1.6631**	**26**	**436**
2.454	**45**	**2.451**	**48**	**620**	**1.6215**	**30**	**1.6226**	**31**	**526**
2.433	7	2.432	2	324	1.5853	2	1.5854	1	824
2.367	9	2.368	7	541	1.5712	5	1.5712	4	327
2.345	5	2.345	3	404	1.5580	7	1.5579	6	616
2.320	8	2.319	7	105	1.5397	2	1.5362	2	735
2.293	5	2.296	5	334	1.5318	1	1.5312	2	626
2.269	2	2.268	2	631	1.5235	4	1.5237	5	942
2.193	5	2.194	9	710	1.5089	2	1.5084	1	1021
2.177	5	2.169	5	701	1.5028	1	1.5029	1	1002
2.158	3	2.164	3	711	1.4979	8	1.4979	5	636
2.141	2	2.143	2	305	1.4753	1	1.4752	2	1022
2.121	11	2.122	14	315					

[1] The eight strongest lines are highlighted bold.

References

1. Deer, W.A.; Howie, R.A.; Zussman, J. *Rock-Forming Minerals: Orthosilicates, Vol 1A*, 1st ed.; Geological Society: London, UK, 1982; pp. 701–719.

2. Gnos, E.; Armbruster, T. Relationship among metamorphic grade, vesuvianite "rod polytypism", and vesuvianite composition. *Am. Mineral.* **2006**, *91*, 862–870. [CrossRef]

3. Olesch, M. Natürliche und synthetische Fe-haltige Vesuviane. *Fortschr. Mineral.* **1979**, *57*, 114–115. (In German)

4. Kappeler, M.A. *Prodromus Crystallographiae de Crystallis Improprie sic Dictis Commentarium*; Heinrich, R.W., Ed.; HR Wyssing: Lucerna, Switzerland, 1723; pp. 1–43.

5. Russo, M.; Punzo, I. *I Minerali del Somma-Vesuvio*, 1st ed.; AMI: Cremona, Italy, 2004; pp. 1–317.

6. Werner, A.G. *Klaproth's Beiträge: Über Vesuvian*; Klaproth, M.H., Ed.; Becker und Compagnie: Berlin, Germany, 1795; pp. 1–34.

7. Clarke, F. The constitution of the silicates. *Bull. U. S. Geol. Surv.* **1895**, *125*, 109–110.

8. Sjögren, H. Analyser pa tvenne vesuvian-varieter och vesuvianens kemiska constitution I Allmänhet. *Geol. I Stockh. Forh.* **1895**, *17*, 267–271. [CrossRef]

9. Weibull, M. Studien über vesuvian. *Z. Krystallogr.* **1896**, *35*, 26–35. [CrossRef]

10. Jannasch, P.; Weingarten, P. Uber die chemische Zusammensetzung und Konstitution des Vesuvians und des Wiluits. *Z. Anorg. Allg. Chem.* **1896**, *11*, 40–48. [CrossRef]

11. Warren, B.E.; Modell, D.I. The structure of vesuvianite $Ca_{10}Al_4(Mg,Fe)_2Si_9O_{34}(OH)_4$. *Z. Kristallogr.* **1931**, *78*, 422–432. [CrossRef]

12. Machatschki, F. Zur Formel des Vesuvian. *Z. Kristallogr.* **1932**, *81*, 148–152. [CrossRef]

13. Coda, A.; Giusta, D.A.; Isetti, G.; Mazzi, F. On the structure of vesuvianite. *Atti Accad. Sci. Torino* **1970**, *105*, 1–22.

14. Groat, L.A.; Hawthorne, F.C.; Ercit, T.S.; Grice, J.D. Wiluite, $Ca_{19}(Al,Mg,Fe,Ti)_{13}(B,Al,\square)_5Si_{18}O_{68}(O,OH)_{10}$, a new mineral species isostructural with vesuvianite, from the Sakha Republic, Russian Federation. *Can. Mineral.* **1998**, *36*, 1301–1304. [CrossRef]

15. Groat, L.A.; Hawthorne, F.C.; Ercit, T.S. The chemistry of vesuvianite. *Can. Mineral.* **1992**, *33*, 19–48.

16. Armbruster, T.; Gnos, E.; Dixon, R.; Gutzmer, J.; Hejny, C.; Döbelin, N.; Medenbach, O. Manganvesuvianite and tweddillite, two new Mn^{3+}-silicate minerals from the Kalahari manganese fields, South Africa. *Mineral. Mag.* **2002**, *66*, 137–150. [CrossRef]

17. Galuskin, E.V.; Galuskina, I.O.; Sitarz, M.; Stadnicka, K. Si-deficient, OH-substituted, boron-bearing vesuvianite from the Wiluy River, Yakutia, Russia. *Can. Mineral.* **2003**, *41*, 833–842. [CrossRef]

18. Britvin, S.N.; Antonov, A.A; Krivovichev, S.V.; Armbruster, T.; Burns, P.C.; Chukanov, N.V. Fluorvesuvianite, $Ca_{19}(Al,Mg,Fe^{2+})_{13}[SiO_4]_{10}[Si_2O_7]_4O(F,OH)_9$, a new mineral species from Pitkäranta, Karelia, Russia: Description and crystal structure. *Can. Mineral.* **2003**, *41*, 1371–1380. [CrossRef]

19. Galuskin, E.V.; Galuskina, I.O.; Dzierżanowski, P. Chlorine in vesuvianites. *Miner. Pol.* **2005**, *36*, 51–61.

20. Hålenius, U.; Bosi, F.; Gatedal, K. Crystal structure and chemistry of skarn-associated bismuthian vesuvianite. *Am. Mineral.* **2013**, *98*, 566–573. [CrossRef]

21. Aksenov, S.M.; Chukanov, N.V.; Rusakov, V.S.; Panikorovskii, T.L.; Gainov, R.R.; Vagizov, F.G.; Rastsvetaeva, R.K.; Lyssenko, K.A.; Belakovskiy, D.I. Towards a revisitation of vesuvianite-group nomenclature: The crystal structure of Ti-rich vesuvianite from Alchuri, Shigar valley, Pakistan. *Acta Crystallogr. B* **2016**, *72*, 744–752. [CrossRef] [PubMed]

22. Panikorovskii, T.L.; Krivovichev, S.V.; Yakovenchuk, V.N.; Shilovkikh, V.V.; Mazur, A.S. Crystal chemistry of Na-bearing vesuvianite from fenitized gabbroid of the Western Keivy (Kola peninsula, Russia). *Zap. Ross. Mineral. Obsh.* **2016**, *145*, 83–95. (In Russian)

23. Panikorovskii, T.L.; Shilovskikh, V.V.; Avdontseva, E.Y.; Zolotarev, A.A.; Pekov, I.V.; Britvin, S.N.; Hålenius, U.; Krivovichev, S.V. Cyprine, $Ca_{19}Cu^{2+}(Al,Mg)_{12}Si_{18}O_{69}(OH)_9$, a new vesuvianite-group mineral from the Wessels mine, South Africa. *Eur. J. Mineral.* **2017**, *29*, 295–307. [CrossRef]

24. Panikorovskii, T.L.; Shilovskikh, V.V.; Avdontseva, E.Y.; Zolotarev, A.A.; Karpenko, V.Y.; Mazur, A.S.; Yakovenchuk, V.N.; Krivovichev, S.V.; Pekov, I.V. Magnesiovesuvianite, $Ca_{19}Mg(Al,Mg)_{12}Si_{18}O_{69}(OH)_9$, a new vesuvianite-group mineral. *J. Geosci.* **2017**, *1*, 25–36. [CrossRef]

25. Panikorovskii, T.L.; Chukanov, N.V.; Aksenov, S.M.; Mazur, A.S.; Avdontseva, E.Y.; Shilovskikh, V.V.; Krivovichev, S.V. Alumovesuvianite, $Ca_{19}Al(Al,Mg)_{12}Si_{18}O_{69}(OH)_9$, a new vesuvianite-group member from the Jeffrey mine, Asbestos, Estrie Region, Québec, Canada. *Mineral. Petrol.* **2017**, *111*, 833–842. [CrossRef]

26. Dyrek, K.; Platonov, A.N.; Sojka, Z.; Żabinski, W. Optical absorption and EPR study of Cu^{2+} ions in vesuvianite ("cyprine") from Sauland, Telemark, Norway. *Eur. J. Mineral.* **1992**, *4*, 1285–1289. [CrossRef]

27. Panikorovskii, T.L.; Krivovichev, S.V.; Zolotarev, A.A.; Antonov, A.A. Crystal chemistry of low-symmetry (*P4nc*) vesuvianite from the Kharmankul' Cordon (South Urals, Russia). *Zap. Ross. Mineral. Obsh.* **2016**, *145*, 94–104. (In Russian)

28. Panikorovskii, T.L.; Krivovichev, S.V; Galuskin, E.V.; Shilovskikh, V.V.; Mazur, A.S.; Bazai, A.V. Si-deficient, OH-substituted, boron-bearing vesuvianite from Sakha-Yakutia, Russia: A combined single-crystal, ^{1}H MAS-NMR and IR spectroscopic study. *Eur. J. Mineral.* **2016**, *28*, 931–941. [CrossRef]

29. Panikorovskii, T.L.; Mazur, A.S.; Bazai, A.V.; Shilovskikh, V.V.; Galuskin, E.V.; Chukanov, N.V.; Rusakov, V.S.; Zhukov, Y.M.; Avdontseva, E.Y.; Aksenov, S.M.; et al. X-ray diffraction and spectroscopic study of wiluite: Implications for the vesuvianite-group nomenclature. *Phys. Chem. Mineral.* **2017**, *44*, 577–593. [CrossRef]

30. Giuseppetti, G.; Mazzi, F. The crystal structure of a vesuvianite with *P*4/*n* symmetry. *Tsch. Mineral. Petrol.* **1983**, *31*, 277–288. [CrossRef]
31. Xu, J.; Li, G.; Fan, G.; Ge, X.; Zhu, X.; Shen, G. Hongheite, IMA 2017-027. CNMNC Newsletter No. 39, October 2017, page 1283. *Mineral. Mag.* **2017**, *81*, 1279–1286.
32. Veblen, D.R.; Wiechmann, M.J. Domain structure of low-symmetry vesuvianite from Crestmore, California. *Am. Mineral.* **1991**, *76*, 397–404.
33. Allen, F.M.; Burnham, C.W. A comprehensive structure-model for vesuvianite: Symmetry variation and crystal growth. *Can. Mineral.* **1992**, *30*, 1–18.
34. Groat, L.A.; Hawthorne, F.C.; Ercit, T.S.; Putnis, A. The symmetry of vesuvianite. *Can. Mineral.* **1993**, *31*, 617–635.
35. Tanaka, T.; Akizuki, M.; Hudoh, Y. Optical properties and crystal structure of triclinic growth sectors in vesuvianite. *Mineral. Mag.* **2002**, *66*, 261–274. [CrossRef]
36. Fitzgerald, S.; Leavens, P.B.; Rossman, G.R.; Yap, G.P.A.; Rose, T. Vesuvianite from Pajsberg, Sweden, and the role of Be in the vesuvianite structure. *Can. Mineral.* **2016**, *54*, 1525–1537. [CrossRef]
37. Nickel, E.H.; Grice, J.D. The IMA Commission on New Minerals and Mineral Names: Procedures and guidelines on mineral nomenclature, 1998. *Can. Mineral.* **1998**, *36*, 913–926. [CrossRef]
38. Balassone, G.; Talla, D.; Beran, A.; Mormone, A.; Altomare, A.; Moliterni, A.; Mondillo, N.; Saviano, M.; Petti, C. Vesuvianite from Somma-Vesuvius volcano (Southern Italy): Chemical, X-ray diffraction and single-crystal polarized FTIR investigations. *Period. Mineral.* **2011**, *80*, 369–384. [CrossRef]
39. Balassone, G.; Bellatreccia, F.; Mormone, A.; Biagioni, C.; Pasero, M.; Petti, C.; Mondillo, N.; Fameli, G. Sodalite-group minerals from the Somma-Vesuvius volcanic complex, Italy: A case study of K-feldspar-rich xenoliths. *Mineral. Mag.* **2012**, *76*, 191–212. [CrossRef]
40. Balassone, G.; Kahlenberg, V.; Altomare, A.; Mormone, A.; Rizzi, R.; Saviano, M.; Mondillo, M. Nephelines from the Somma-Vesuvius volcanic complex (Southern Italy): Crystal chemical, structural and genetic investigations. *Mineral. Petrol.* **2014**, *108*, 71–90. [CrossRef]
41. Balassone, G.; Bellatreccia, F.; Ottolini, L.; Mormone, A.; Petti, C.; Ghiara, M.R.; Altomare, A.; Saviano, M.; Rizzim, R.; D'oraziom, L. Sodalite-group minerals from Somma-Vesuvius volcano (Naples, Italy): A combined EPMA, SIMS and FTIR crystal chemical study. *Can. Mineral.* **2016**, *54*, 583–604. [CrossRef]
42. Gilg, A.H.; Lima, A.; Somma, R.; Belkin, H.E.; De Vivo, B.; Ayuso, R.A. Isotope geochemistry and fluid inclusion study of skarns from Vesuvius. *Mineral. Petrol.* **2001**, *73*, 145–176. [CrossRef]
43. Hermes, O.D.; Cornell, W.C. Petrochemical significance of xenolithic nodules associated with potash-rich lavas of Somma-Vesuvius volcano. In *NSF Final Technical Report*; University Rhode Island: Kingston, RI, USA, 1978; p. 58.
44. Joron, J.L.; Metrich, N.; Rosi, M.; Santacroce, R.; Sbrana, A. Chemistry and petrography. *CNR Quad. Ric. Sci.* **1987**, *114*, 105–174.
45. Gruppo Mineralogico Geologico Napoletano. Available online: http://www.gmgn.it/index.html (accessed on 1 November 2017).
46. Sheldrick, G.M. A short history of SHELX. *Acta Crystallogr. A* **2008**, *64*, 112–116. [CrossRef] [PubMed]
47. Agilent Technologies. *CrysAlis CCD and CrysAlis RED*; Oxford Diffraction Ltd.: Oxfordshire, UK, 2014.
48. Elmi, C.; Brigattim, M.F.; Pasqualim, L.; Montecchi, M.; Laurora, A.; Malferrari, D.; Nannarone, S. High-temperature vesuvianite: Crystal chemistry and surface considerations. *Phys. Chem. Miner.* **2011**, *38*, 459–468. [CrossRef]
49. Żabiński, W.; Wactawska, Z.; Paluszkiewicz, C. Thermal decomposition of vesuvianite. *J. Therm. Anal.* **1996**, *46*, 1437–1447. [CrossRef]
50. Foldvari, M. *Handbook of Thermogravimetric System of Minerals and Its Use in Geological Practice*; Geological Institute of Hungary: Budapest, Hungary, 2011; pp. 1–180.
51. Phillips, B.L.; Allen, F.M.; Kirkpatrick, R.J. High-resolution solid-state ^{27}Al NMR spectroscopy of Mg-rich vesuvianite. *Am. Mineral.* **1987**, *72*, 1190–1194.
52. Olejniczak, Z.; Żabiński, W. ^{27}Al NMR study of white vesuvianite from Piz Lunghin, Switzerland. *Miner. Pol.* **1996**, *27*, 41–45.
53. Yesinowski, J.P.; Eckert, H.; Rossman, G.R. Characterization of hydrous species in minerals by high-speed ^{1}H MAS-NMR. *J. Am. Chem. Soc.* **1988**, *110*, 1367–1375. [CrossRef]

54. Lager, G.A.; Xie, Q.; Ross, F.K.; Rossman, G.R.; Armbruster, T.; Rotella, F.J.; Schultz, A.J. Hydrogen-atom position in *P*4/*nnc* vesuvianite. *Can. Mineral.* **1999**, *37*, 763–768.

55. Ohkawa, M.; Yoshiasa, A.; Takeno, S. Crystal chemistry of vesuvianite: Site preferences of square-pyramidal coordinated sites. *Am. Mineral.* **1992**, *77*, 945–953.

56. Ohkawa, M.; Armbruster, T.; Galuskin, E. Structural investigation of low symmetry vesuvianite collected from Tojyo, Hiroshima, Japan: Implications for hydrogarnet-like substitution. *J. Mineral. Petrol. Sci.* **2009**, *104*, 69–76. [CrossRef]

57. Pavese, A.; Prencipe, M.; Tribaudino, M.; Aagaard, S.S. X-ray and neutron single-crystal study of *P*4/*n* vesuvianite. *Can. Mineral.* **1998**, *36*, 1029–1037.

58. Armbruster, T.; Gnos, E. "Rod" polytypism in vesuvianite: Crystal structure of a low-temperature *P*4*nc* with pronounced octahedral cation ordering. *Schweiz. Mineral. Petrogr.* **2000**, *80*, 109–116.

59. Galuskin, E.V. *Vesuvianite-Group Minerals from Achtarandite Rocks (Wiluy River, Yakutia)*, 1st ed.; University of Silesia: Katowice, Poland, 2005; pp. 123–137. (In Polish)

60. Kraczka, J.; Żabiński, W. Mössbauer study of iron in some vesuvianites. *Mineral. Pol.* **2003**, *34*, 37–44.

61. Rusakov, V.S.; Kovalchuk, R.V.; Borovikova, E.Y.; Kurazhkovskaya, V.S. State of iron atoms in high vesuvianites according to Mössbauer spectroscopy data. *Zap. Ross. Mineral. Obsh.* **2006**, *135*, 91–100. (In Russian)

62. Manning, P.G.; Tricker, M.J. Optical absorption and Mössbauer spectral studies of iron and titanium site-populations in vesuvianites. *Can. Mineral.* **1975**, *13*, 259–265.

63. Groat, L.A.; Evans, R.J.; Cempírek, J.; McCammon, C.; Houzar, S. Fe-rich and As-bearing vesuvianite and wiluite from Kozlov, Czech Republic. *Am. Mineral.* **2013**, *98*, 1330–1337. [CrossRef]

64. Bruker AXS. *Topas V4.2: General Profile and Structure Analysis Software for Powder Diffraction Data*; Bruker AXS GmbH: Karlsruhe, Germany, 2009.

65. Groat, L.A.; Evans, R.J. Crystal chemistry of Bi- and Mn-bearing vesuvianite from Langban, Sweden. *Am. Mineral.* **2012**, *97*, 1627–1634. [CrossRef]

66. Fitzgerald, S.; Leavens, P.B.; Rheingold, A.L.; Nelen, J.A. Crystal structure of a REE-bearing vesuvianite from San Benito County, California. *Am. Mineral.* **1987**, *72*, 625–628.

67. Galuskin, E.V.; Galuskina, I.O.; Stadnicka, K.; Armbruster, T.; Kozanecki, M. The crystal structure of Si-deficient, OH-substituted, boron-bearing vesuvianite from the Wiluy River, Sakha-Yakutia, Russia. *Can. Mineral.* **2007**, *45*, 239–248. [CrossRef]

68. Groat, L.A.; Hawthorne, F.C.; Rossman, G.R.; Scott, T.E. The infrared spectroscopy of vesuvianite in the OH region. *Can. Mineral.* **1995**, *33*, 609–626.

69. Chukanov, N.V.; Panikorovskii, T.L.; Chervonnyi, A.D. On the relationships between crystal-chemical characteristics of vesuvianite-group minerals and their IR spectra. *Zap. Ross. Mineral. Obsh.* **2017**, in print. (In Russian)